Chapter

BAC Photobleaching in Bismuth-Doped and Bismuth/Erbium Co-Doped Optical Fibers

Bowen Zhang, Mingjie Ding, Shuen Wei, Binbin Yan, Gang-Ding Peng, Yanhua Luo and Jianxiang Wen

Abstract

Bismuth-doped optical fiber (BDF) and bismuth/erbium co-doped optical fiber (BEDF) have attracted much attention due to their ultra-broadband luminescence in the near-infrared (NIR) region. The photobleaching effect on bismuth active centers (BACs) related to the NIR luminescence has been systematically investigated and summarized, in terms of irradiation intensity, irradiation wavelength, and temperature. All these findings not only give the deep insights into the fundamental structure of BACs but also provide an effective way to control the BACs. They play an important role for the development of BDF- and BEDF-based devices with high performance and stability under laser exposure in future.

Keywords: bismuth-doped optical fiber (BDF), bismuth/erbium co-doped optical fiber (BEDF), bismuth active center (BAC), laser irradiation, photobleaching, irradiation intensity, irradiation wavelength, temperature

1. Introduction

Since Fujimoto et al. in 1999 first demonstrated that bismuth-doped silica glass could generate broadband luminescence covering the near-infrared (NIR) region [1], the bismuth-doped materials have attracted considerable attention due to their ultra-wide luminescence [2–8]. Especially, the bismuth-doped and bismuth/erbium co-doped optical fibers (BDFs and BEDFs) have been developed for tunable fiber laser, amplifier, and ultra-broadband light source operating in the range from 1000 to 1800 nm [9–15].

Although great endeavor has been made to improve the performance of BDFs and BEDFs, challenges still exist, and they have become obstacles to many practical applications. One of the key challenges is that the fundamental structure of bismuth active centers (BACs) and the nature of their NIR luminescence remain unclear. Based on the previous researches, it was generally accepted that the formation of BACs greatly depends on the material compositions [12, 15]. With different doping elements such as aluminum, phosphorus, silicon and germanium in the glass environment, there are four types of BACs in the BDFs, namely BAC associated with aluminum (BAC-Al), BAC associated with phosphorus (BAC-P), BAC associated with silicon (BAC-Si),

and BAC associated with germanium (BAC-Ge), respectively [16–19]. Multiple absorption peaks of these BACs have been observed in BDFs and BEDFs, for example, BAC-Al (510, 700, and 1050 nm), BAC-P (460, 750, and 1300 nm), BAC-Si (420, 830, and 1400 nm), and BAC-Ge (463, 925, and 1600 nm) [17, 18]. The typical NIR luminescence bands of these BACs locate at ~1100 nm (BAC-Al), ~1300 nm (BAC-P), ~1400 nm (BAC-Si), and ~ 1700 nm (BAC-Ge), respectively [15, 17].

To better reveal the nature of the NIR luminescence in BDFs/BEDFs and the configuration of BACs, various post treatments, such as ionizing radiation, laser irradiation, and thermal treatment, have already been applied [20–25]. Thereinto, as a result of laser irradiation, the photobleaching of BDFs/BEDFs leading to the gradual decay of the luminescence of BACs is quite obvious. In this chapter, the photobleaching effect on BACs observed in BDFs and BEDFs has been reviewed. More specially, this effect is demonstrated and analyzed in detail from the angle of BAC type, irradiation intensity, irradiation wavelength, and temperature. In addition, the photobleaching mechanism for each BAC is also discussed. The investigation of this photobleaching process gives not only the deep insights into the structure of BACs but also more information of photostability of BDFs/BEDFs. With further understanding of the BACs, it helps to develop an effective way to control the BACs and obtain better and more stable optical performance of BDF and BEDF for practical applications.

2. Phenomenon of photobleaching

The photobleaching effect observed in some luminescent materials is featured by the gradual decay of luminescence after laser irradiation. This effect can be referred as a process of laser irradiation-induced luminous centers destruction and/or converting into the nonluminous center. This process is called the photobleaching effect [26].

The photobleaching effect has been found in many materials. For example, it was reported that the green fluorescent protein could be bleached under laser irradiation [27]. The Sm^{2+} emission in epitaxial CaF_2 film could be bleached partially under 633-nm irradiation [28]. The similar photoinduced reduction of luminescence has also been observed in Nd^{3+}:$LiYF_4$ and YVO_4:Bi^{3+}/Eu^{3+} nanoparticles [29, 30]. In addition, a large number of dyes present the photobleaching characteristics [31–34]. In general, the photobleaching effect is caused by breaking of covalent bonds or nonspecific reactions between the luminous center and surrounding molecules. Especially, some photobleaching-based techniques such as fluorescence loss in photobleaching and fluorescence recovery after photobleaching have been developed and used for molecular marker, in vivo cell tracking, and investigation of molecule diffusion in biology [27, 35–37].

The photobleaching effect also exists in the glass materials. Exposure to 977 nm light irradiation led to the absorption decrease of Yb^{3+} in ytterbium-doped silica fiber [38]. In addition, the darkened Yb-doped fiber could be photobleached when irradiated by 355 and 633 nm laser [39, 40]. The similar photobleaching effect has also been observed in the thulium-doped fibers [41].

As for the bismuth-doped materials, the BAC-related NIR luminescence was reduced under laser irradiation in bismuth-doped silica-based glasses, $TlCdCl_3$ crystal and $Sr_2B_5O_9Cl$:Bi crystal [42–44]. In the case of BDFs/BEDFs, a number of studies on the photobleaching of various BACs have been reported [19, 21, 45–54]. Herein, the photobleaching effect on BAC-Si, BAC-Ge, BAC-Al, and BAC-P in BDFs and BEDFs is demonstrated in relation to irradiation intensity, irradiation wavelength, and temperature, respectively. The underlying mechanisms of these photobleaching effects in BDFs and BEDFs are also discussed below.

3. Photobleaching of BAC-Si

The photobleaching of BAC-Si in BEDF under 830-nm laser irradiation has been reported in [46]. By the 830 nm laser irradiation with an intensity of 0.12 MW/cm^2, the luminescence spectra of 50 cm BEDF at different irradiation time were shown in **Figure 1a**. It is evident that the NIR luminescence of BAC-Si peaking at ~1420 nm decreases continuously with the longer exposure time. In addition, the absorption of BAC-Si peaking at ~816 nm demonstrates the similar trend, gradually decaying when exposed to the 830 nm laser as shown in **Figure 1b**. The decrease of both the NIR luminescence and absorption clearly indicates the degradation of BAC-Si. Interestingly, after the irradiation, both the absorption and luminescence of BAC-Si gradually recover to the initial value in 48 hours at room temperature (RT). This recovery behavior implies that the photobleaching of BAC-Si under 830-nm irradiation in BEDF is reversible in the mild condition.

To characterize the photobleaching effect on BAC-Si, the stretched exponential function (SEF) has been used, which is expressed as [55]:

$$I(t) = I_1 + (I_0 - I_1)e^{-\left(\frac{t}{\tau}\right)^{\beta}} \tag{1}$$

where I_1 and I_0 are the luminescence intensities at bleaching saturated time and initial time, τ represents the bleaching time and β stands for the stretched parameter. In addition, the bleaching ratio r_B, defined by bleached part of the luminescence (I_0–I_1) divided by the initial luminescence before irradiation (I_0), is used to quantify the photobleaching degree [47]. **Figure 2** shows the typical luminescence variation at 1420 nm irradiated by 0.12 MW/cm^2 830-nm laser, which is well fitted by SEF in Eq. (1).

3.1 Irradiation intensity dependence

It has been found that the irradiation intensity (power) has a significant effect on the photobleaching of BACs. Higher irradiation intensity provides more photons, which may lead to stronger photobleaching effect. The irradiation intensity dependence of photobleaching of BAC-Si in BEDF was investigated under 830-nm laser irradiation, and the variation of irradiation intensity was achieved by changing the incident power ranged from 0.39 to 35 mW [47]. **Figure 3a** demonstrates the time

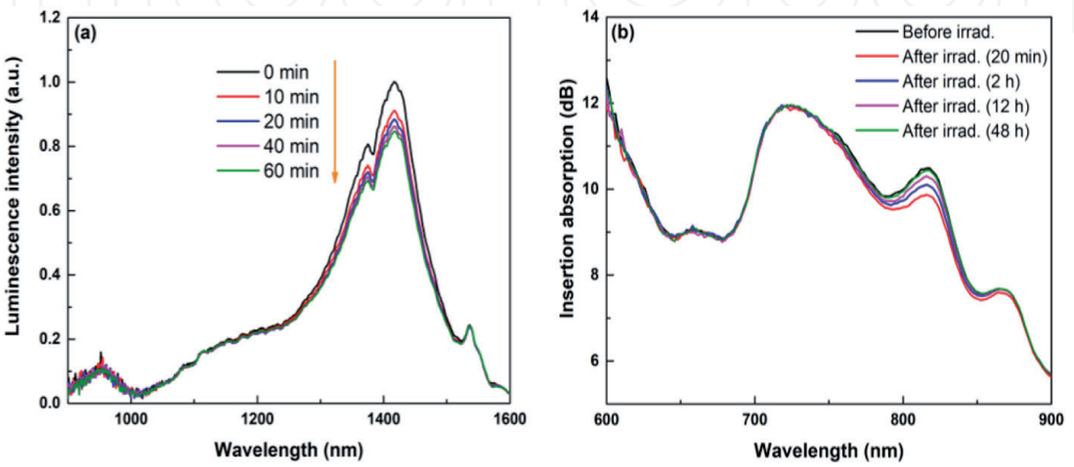

Figure 1.
(a) Luminescence spectra of the BEDF under 830-nm irradiation in 60 minutes of exposure time; (b) BEDF insertion absorption spectra before and after irradiation (20 minutes to 48 hours) [46].

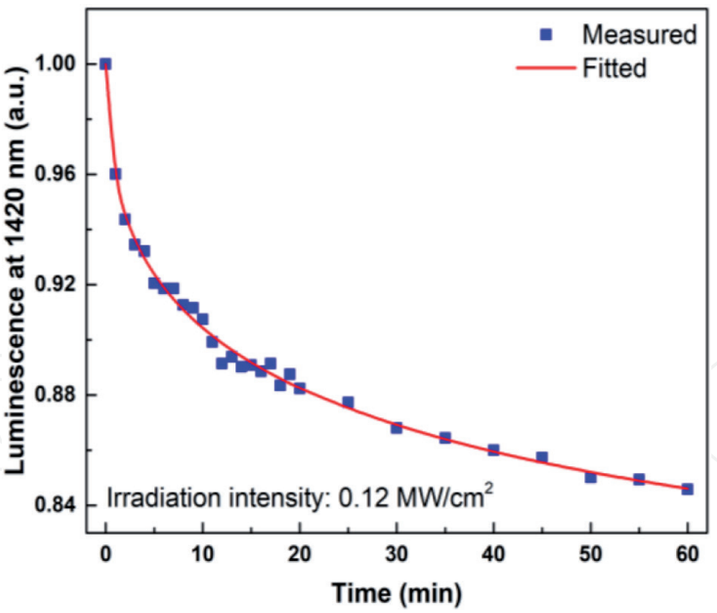

Figure 2.
Variation of luminescence intensity at 1420 nm as a function of irradiation time [46].

evolution of BAC-Si luminescence at 1420 nm under different irradiation power. It is obvious that the luminescence of BAC-Si decays more severely as the irradiation power increases. Furthermore, the luminescence at 1420 nm, time constant $1/\tau$, and bleaching ratio r_B vs. irradiation power is plotted as **Figure 3b**. It is worth noting that both the bleaching ratio and bleaching rate tend to be saturated as the irradiation power increases. Such trend is similar with the variation trend of luminescence at 1420 nm. It hints that the excitation of BAC-Si may participate in the photobleaching process.

3.2 Irradiation wavelength dependence

The photobleaching of BAC-Si was observed in BEDF under 710 and 1380 nm irradiation. As shown in **Figure 4**, the luminescence of BAC-Si is significantly bleached under irradiation of 710 nm, but almost no change under 980-nm irradiation. The inset of **Figure 4** indicates that the BAC-Si luminescence can be slightly bleached under 1380-nm irradiation, which is much weaker than that 710 nm irradiation. In addition, the luminescence of BAC-Si in BDF can be bleached under 532- and 407-nm irradiation [45]. The photobleaching effect on BAC-Si with different irradiation wavelengths is further summarized and listed in **Table 1**. Seen from **Table 1**, except for 980 nm, the photobleaching of BAC-Si can be obtained under all the other applied irradiation wavelengths even the irradiation intensity for some wavelengths is quite small. Generally, it is believed that the shorter wavelength provides larger photon energy. With the increasing photon energy, a greater number of BACs are degraded, resulting in the stronger photobleaching effect. However, even though light at 980 nm has more photon energy than that at 1380 nm, no obvious photobleaching effect is observed under 980-nm irradiation. Considering the fact that 980 nm is unable to excite BAC-Si to the upper energy level, therefore, it is suggested that the photobleaching effect on BAC-Si can only happen when the irradiation wavelength is capable of pumping BAC-Si to excited state. The detailed mechanism will be discussed in Section 3.4.

3.3 Temperature dependence

The temperature dependence of photobleaching effect on BAC-Si in BEDF was studied in the range from 77 to 673 K [47]. The bleaching ratio of BAC-Si under

0.36 MW/cm^2 830-nm irradiation as a function of temperature is plotted as **Figure 5**. As the temperature rises from 77 to 673 K, the bleaching ratio of BAC-Si increases from 34 to 66% and then tends to be saturated. This result indicates that the heating of BEDF

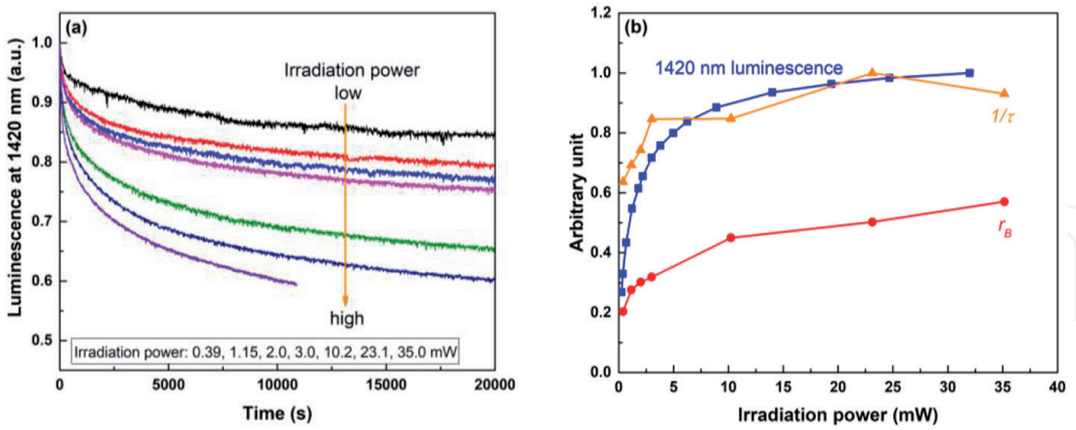

Figure 3.
(a) Evolution of BAC-Si luminescence at 1420 nm under different irradiation power; (b) luminescence, time constant, and bleaching ratio vs. irradiation power [47].

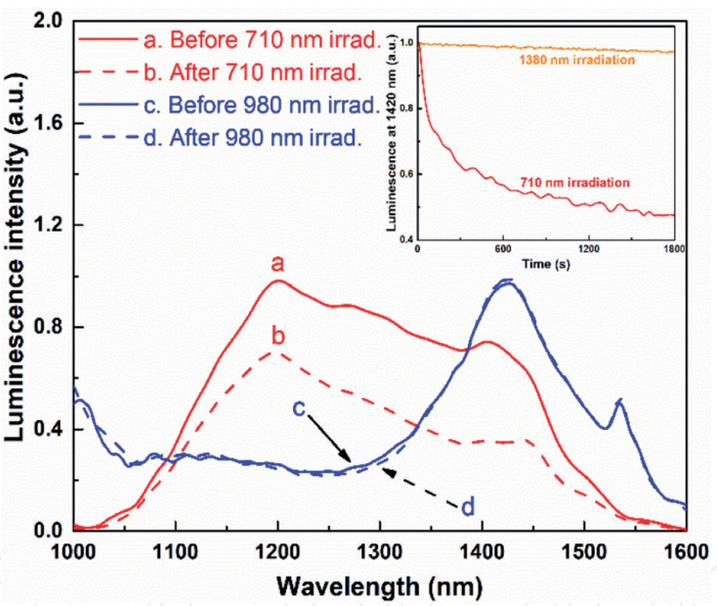

Figure 4.
Luminescence spectra excited by 0.2 mW 830-nm laser before and after 710- and 980-nm irradiation. The inset presents the variation of luminescence at 1420 nm with irradiation wavelengths of 710 and 1380 nm [47].

Sample	Irradiation λ (nm)	Intensity (MW/cm^2)	r_B	Ref.
BDF	407	1	0.85	[45]
BDF	532	1.5	0.8	[45]
BEDF	710	0.36	0.55	[47]
BEDF	830	0.36	0.57	[47]
BEDF	980	0.36	—	[47]
BEDF	1380	0.005	0.06	[47]

Table 1.
Summary of irradiation wavelength influence upon photobleaching of BAC-Si.

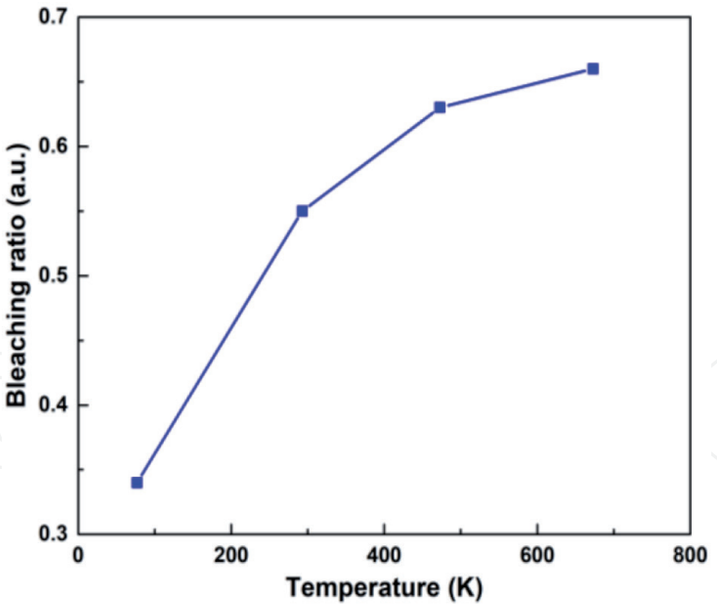

Figure 5.
Temperature dependence of bleaching ratio of BAC-Si under 0.36 MW/cm² 830-nm irradiation [47].

to the high temperature can accelerate the electron movement, leading to the stronger photobleaching of BAC-Si.

3.4 Photobleaching mechanism of BAC-Si

Based on the fact that the excitation of BAC-Si is an essential condition for the photobleaching [47], the photobleaching process is deduced to be expressed as:

$$Bi_{BAC-Si}^{+x} \xrightarrow{h\nu} {}^{*}Bi_{BAC-Si}^{+x} \xrightarrow{kT} Bi_{BAC-Si}^{+(x+1)} + e^{-}, \tag{2}$$

where Bi_{BAC-Si}^{+x} stands for the Bi ion in a BAC-Si with a valence state of +x, '*' symbolizes the excited state of the active center, and $h\nu$ and kT are the photon energy and thermal energy, respectively. As shown by Eq. (2), the photobleaching mechanism of BAC-Si can be described as: first, the Bi ions absorb the 830 nm photons and are pumped to the upper excited state corresponding to 816 nm; second, with the help of thermal energy, some Bi ions release the electrons which are seized by the surrounding material defects (e.g., self-trapped holes, STH), arousing the decay of luminescence and absorption. As seen from **Table 1**, the BAC-Si could also be bleached under 1380-nm irradiation with a slight bleaching ratio of 0.06. The Bi ions absorb 1380 nm photons and then are excited to the lower excited state, and then the electrons can transfer from a small part of Bi ions at the lower excited state to the nearby defects. Compared with Bi ions at the upper excited state, this electron movement pathway at the lower excited state is more difficult.

4. Photobleaching of BAC-Ge

Photobleaching of BAC-Ge has been found in bismuth-doped optical germanosilicate fibers [45]. After 30 minutes' irradiation of 532-nm laser with an intensity of 1.2 MW/cm^2, both the absorption and the luminescence related to BAC-Ge significantly change as shown by the absorption and luminescence spectra of BDF before and

after the irradiation. The dramatical decrease of absorption at 925 and 1650 nm and luminescence at 1700 nm clearly indicate the destruction (photobleaching) of BAC-Ge.

The photobleaching of BAC-Ge can also be fitted well by SEF in Eq. (1). The variation of luminescence at 1700 nm excited by 1550 nm under 532-nm irradiation has been demonstrated in [19, 45]. The decay curve of BAC-Ge luminescence at 1700 nm shows the exponential trend. Moreover, there is no recovery behavior after the photobleaching at RT. However, by thermal annealing of the bleached BDF, BAC-Ge could be recovered [19, 45, 53]. After 532-nm laser irradiation, the luminescence of BAC-Ge almost disappears. Annealing the bleached BDF at 600°C, the luminescence of BAC-Ge at ~1700 nm significantly increases, even more than the pristine value, as shown in **Figure 6**. The evident increase of the luminescence of BACs by thermal treatment has been observed in unirradiated BDFs and BEDFs [22, 24, 25, 56–59]. All these results indicate that the thermal treatment can not only lead to the recovery of irradiated fibers but also activate the new BACs.

4.1 Irradiation intensity dependence

The irradiation intensity dependence of photobleaching of BAC-Ge has been studied under 532-nm irradiation with intensity ranged from 0.5 to 2 MW/cm^2 [48]. The bleaching rate $1/\tau$ calculated by the SEF as a function of irradiation power under 532-nm irradiation is plotted as **Figure 7**. Seen from **Figure 7**, the relationship between the bleaching rate and irradiation power in log-log scale is almost linear with a slope of ~1.7. The fitting slope is close to 2, which suggests that the photobleaching of BAC-Ge under 532-nm irradiation is likely to be a two-photon process. In addition, the bleaching rate increases with the irradiation intensity, indicating that more photons obtained by higher irradiation intensity results in faster photobleaching of BAC-Ge.

4.2 Irradiation wavelength dependence

The irradiation wavelength dependence of photobleaching of BAC-Ge differs from that of BAC-Si. As mentioned above, the photobleaching of BAC-Si only happens when the irradiation photon is able to excite BAC-Si. The photobleaching

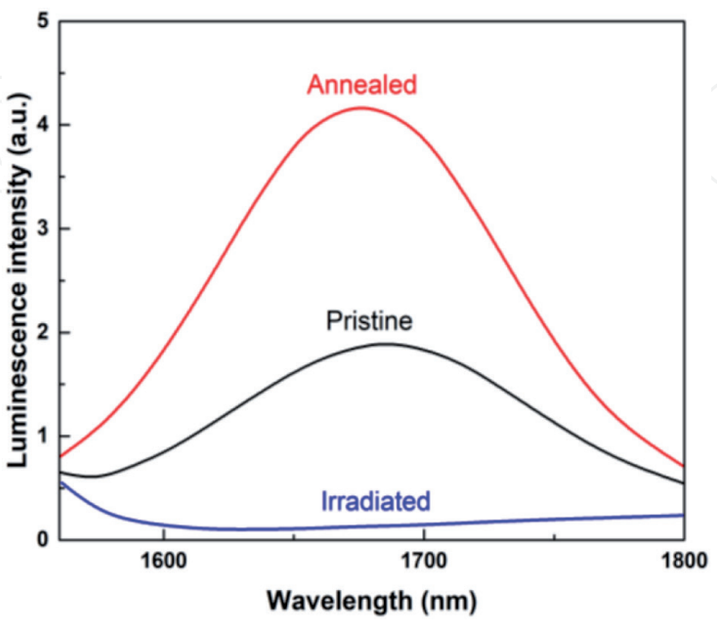

Figure 6.
Evolution of photoluminescence spectra of a BDF at different stages of the experiment: Pristine, irradiated, and annealed [19, 53].

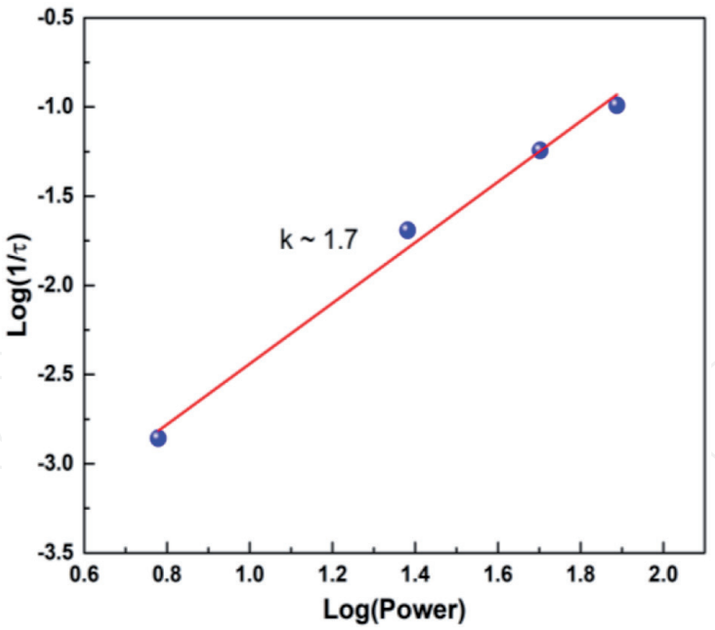

Figure 7.
Bleaching rate as a function of irradiation power under 532-nm irradiation (log-log scale) [48].

of BAC-Ge in BDFs has been observed when irradiated by 244, 407, 532, 639, 975, and 1460 nm [21, 45, 48, 51, 53]. In [48], the variation of BAC-Ge luminescence at 1700 nm in BDF under irradiation at different wavelengths with the irradiation intensity kept at ~0.5 MW/cm^2 has been demonstrated. Clearly, shorter irradiation wavelength provides higher photon energy, leading to stronger photobleaching of BAC-Ge. From this result, the photobleaching of BAC-Ge is almost unrelated to the resonant radiation wavelength. The mechanism of photobleaching of BAC-Ge will be discussed in detail in Section 4.4, which may be different from that of BAC-Si.

4.3 Temperature dependence

The temperature also has an influence upon the photobleaching of BAC-Ge. The BDF was irradiated under 532 nm with an intensity of 0.5 MW/cm^2 at room temperature (300 K) and liquid nitrogen temperature (77 K), respectively [48]. Seen from **Figure 8**, the photobleaching of BAC-Ge is suppressed significantly when the temperature is cooled down to 77 K. It is noticeable that the photoionization of the germanium-related oxygen deficient center (GeODC) decreases at low temperature [60]. Especially, it has already been confirmed that the BAC in bismuth-doped materials should be some cluster making up of Bi ion with the oxygen deficiency center (ODC) rather than Bi ions themselves [61]. Therefore, it is reasonable to deduce that the photobleaching of BAC-Ge may be related to the photoionization of GeODC. It was also found that the 1550-nm laser had no photobleaching effect upon BAC-Ge under 80°C but was able to bleach BAC-Ge when the temperature of BDF was elevated to hundreds of degrees [54]. Such combined effect of thermal treatment and laser irradiation on BAC-Al has also been observed in BEDF [52].

4.4 Photobleaching mechanism of BAC-Ge

It is known that the most convincing model of the nature of BAC is a Bi ion close to a structural defect, and the defect is most probably to be an ODC [62]. Furthermore, the mechanism of photobleaching of BAC-Ge is assumed to be the photoionization of GeODC. The photobleaching process of BAC-Ge induced by the destruction of GeODC by laser irradiation can be expressed as follows:

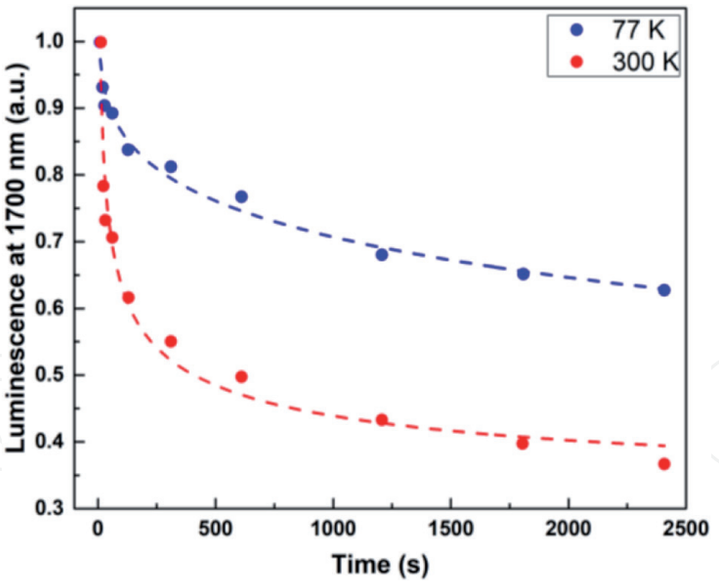

Figure 8.
Variation of BAC-Ge luminescence at 1700 nm in BDF irradiated by 532 nm at 300 and 77 K [48].

$$BAC \equiv \left(Bi^{+n} + ODC\right) \xrightarrow{2h\nu} Bi^{+n} + e^{-} + E' center \tag{3}$$

The hypothesis is supported by the following facts: (1) the irradiation intensity dependence of bleaching rate demonstrates that photobleaching of BAC-Ge is likely to be a two-photon process [48]; (2) the GeODC can be photoionized under UV light irradiation [63]; and (3) the behavior of photobleaching of BAC-Ge is similar to the photoionization of GeODC at low temperature [48].

These results also suggest that the Bi ion adjacent to the ODC is the credible structure of BAC. According to this mechanism, it is believed that the number of the GeODC in the fiber should have an impact on the photobleaching of BAC-Ge. In this case, the doping concentration of Ge may affect the formation of GeODC, resulting in different photobleaching phenomena with various core compositions in [21]. This doping concentration dependence of photobleaching effect may also apply to the photobleaching of BAC-Si, BAC-Al, and BAC-P.

In addition, it is worth noting that the photobleaching of BAC-Si under 532-nm irradiation can be explained utilizing this hypothesis [45]. Therefore, more than one mechanism of photobleaching of BACs under different irradiation wavelengths should exist.

5. Photobleaching of BAC-Al

Compared with BAC-Si and BAC-Ge, the understanding of the fundamental structure of BAC-Al is still limited. A number of studies on photobleaching of BAC-Al have been taken to explore the nature of BAC-Al. It has been reported that the BAC-Al can be bleached with various irradiation conditions in bismuth/erbium co-doped aluminosilicate fibers [49]. **Figure 9** shows the absorption spectra of BEDF in the range from 650 to 750 nm before and after the irradiation. It is clear that the absorption of BAC-Al at ~700 nm decreases after the irradiation of 532, 633, 710, and 830 nm laser (for irradiation at 980 nm, the bleaching effect is not that obvious.). Unlike BAC-Si, after the irradiation, there is no obvious recovery behavior of BAC-Al at RT. Even the bleached BEDF is annealed at high temperatures; there remains no observable recovery of BAC-Al.

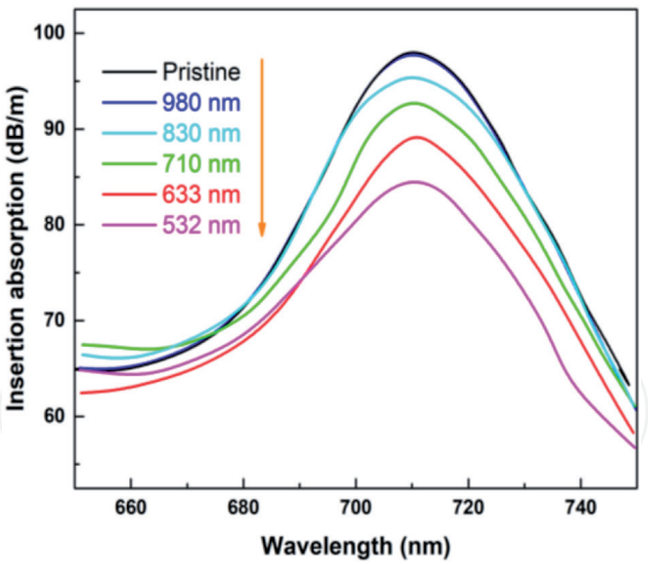

Figure 9.
Absorption of BEDF before and after irradiation at various wavelengths [49].

5.1 Irradiation intensity dependence

The photobleaching of BAC-Al also largely depends on the irradiation intensity [49, 52]. The intensity dependence of photobleaching of BAC-Al under 532-nm irradiation has been demonstrated in [49]. As irradiation intensity increases from 0.06 to 0.16 MW/cm^2, both the bleaching rate and bleaching ratio increase, indicating a faster and stronger photobleaching process. Moreover, the irradiation power dependence of bleaching rate in log-log scale shows a linear trend with a slope of ~1.8, as shown in **Figure 10**. The fitting slope close to 2 also demonstrates that the photobleaching of BAC-Al under 532-nm irradiation is likely to be a two-photon process.

5.2 Irradiation wavelength dependence

The BAC-Al can be bleached under irradiation at both resonant and nonresonant wavelengths. The different irradiation wavelengths (532, 633, 710, 830, and 980 nm) have been applied for the investigation of the photobleaching of Al-doped BEDF [49]. At RT, there is no obvious reduction of BAC-Al luminescence under 980-nm irradiation while the photobleaching of BAC-Al takes place under irradiation of all the other wavelengths. Especially, the stronger photobleaching of BAC-Al can be obtained by increasing the photon energy (reducing the irradiation wavelength) with a growth of the bleaching rate and a reduction of the unbleached ratio as shown in **Figure 11**. This irradiation wavelength dependence suggests that the Al-related ODC (AlODC) may take part in the photobleaching process instead of the Bi ion.

5.3 Temperature dependence

Similar to the BAC-Si and BAC-Ge, the photobleaching of BAC-Al is suppressed at low temperature. It has been reported that the bleaching ratio of BAC-Al under 0.12 MW/cm^2 532-nm irradiation is reduced from 10 to 5% as the temperature falls down from RT to 77 K [49]. In addition, the temperature aggravated photobleaching of BAC-Al has been observed in BEDF [52]. Under 0.34 MW/cm^2 980-nm irradiation, the BAC-Al luminescence at 1191 nm has little change at 293 K but decreases obviously at higher temperatures (423–623 K). The bleaching ratio of BAC-Al dramatically increases with the rising temperature, especially at 623 K, up to 35% of luminescence is bleached, as shown in **Figure 12**. The increasing temperature provides more

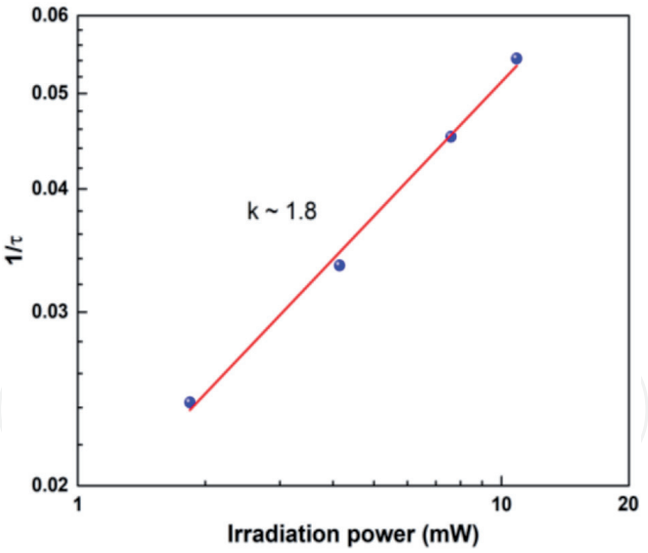

Figure 10.
The bleaching rate 1/τ of BAC-Al in BEDF under 532-nm irradiation versus irradiation power [49].

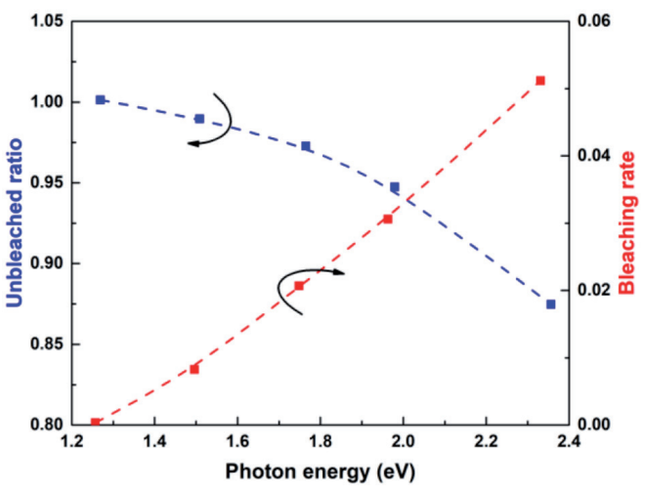

Figure 11.
Unbleached ratio and bleaching rate as a function of the photon energy [49].

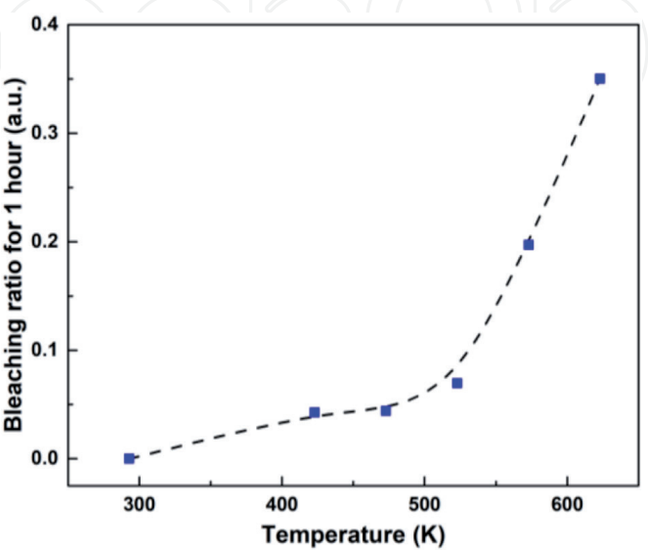

Figure 12.
Bleaching ratio of BAC-Al under 1 hour of 0.3 MW/cm² 980-nm irradiation as a function of the temperature [52].

thermal energy, making it possible for the electron to escape from the BAC-Al. The results imply the strong temperature dependence of photobleaching of BAC-Al, indicating the important role of thermal energy in the photobleaching process.

5.4 Photobleaching mechanism of BAC-Al

Considering that the BAC-Al can be bleached under irradiation of both resonant and nonresonant wavelengths, it is believed that the degradation of BAC-Al under irradiation is due to the photoinduced effects on AlODCs [49], which is much similar with BAC-Ge. Subsequently, the electron released from the AlODC is captured by the nearby defects, arousing the destruction of BAC-Al. In addition, the suppression of photobleaching of BAC-Al at the low temperature arising from the decreasing phonon-assisted rate for relaxation of AlODC, and the electron movement may support the view of participation of AlODC. However, unlike GeODC, the information of photo-ionization of AlODC is still limited, and there may exist more than one mechanism of photobleaching of BAC-Al. Therefore, the mechanism of photobleaching of BAC-Al still needs further investigation for deep understanding of the origin of BAC-Al.

6. Photobleaching of BAC-P

Only one photobleaching relevant study on the BAC-P has been reported so far. The study demonstrates that the luminescence of BAC-P at 1300 nm in BDF can be bleached under 1 MW/cm^2 407-nm irradiation [45]. The evolution of the luminescence of BAC-P is plotted as **Figure 13**, which is possibly linked with P-related ODC (PODC). Of course, more investigation on photobleaching of BAC-P needs to be taken in terms of irradiation intensity, irradiation wavelength, and temperature dependences to get in-depth knowledge of the photobleaching of BAC-P and its structure.

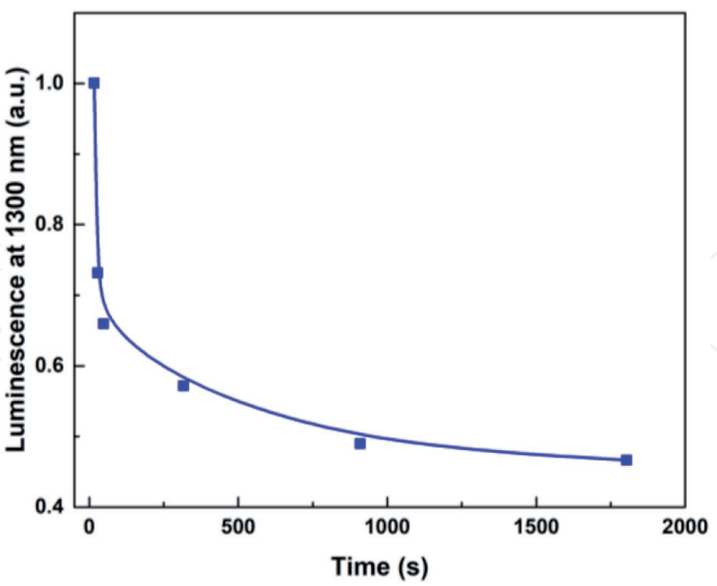

Figure 13.
Evolution of BAC-P luminescence at 1300 nm in BDF under 407-nm irradiation with an intensity of ~1 MW/cm² at room temperature [45].

7. Inductive analysis

The photobleaching effect exists in all four types of BACs. Since photobleaching effect varies case by case and is largely dependent on the irradiation conditions,

Fiber	Core composition	BAC type	Irradiation λ	Intensity	*T*	Time	r_B	Ref.
			nm	MW/cm^2	K	minutes		
BEDF	SiO_2-Al_2O_3-GeO_2-P_2O_5-Er_2O_3-Bi_2O_3 (~0.1 at%)	BAC-Si	830	0.004–0.36	300	360	0.2–0.57	[47]
BDF	10GeO_2– 90SiO_2: Bi	BAC-Si	407 532	1 1.5	300	30	0.85 0.8	[45]
BEDF	SiO_2-Al_2O_3-GeO_2-P_2O_5-Er_2O_3-Bi_2O_3 (~0.1 at%)	BAC-Si	980, 830, 710, 1380	0.36 0.005	300	—	0–0.66 0.06	[47]
BEDF	SiO_2-Al_2O_3-GeO_2-P_2O_5-Er_2O_3-Bi_2O_3 (~0.1 at%)	BAC-Si	830	0.36	77–673	—	0.34–0.66	[47]
BDF	50GeO_2–50SiO_2: Bi (<0.1 mol%)	BAC-Ge	532	0.6–1.2	300	60	—	[21]
BDF	95GeO_2–5SiO_2: Bi (<0.1 mol%)	BAC-Ge	532	0.6–1.2	300	60	—	[21]
BDF	50GeO_2–50SiO_2: Bi (<0.1 mol%)	BAC-Ge	244	—	300	—	1	[51]
BDF	50GeO_2–50SiO_2: Bi (~100 ppm)	BAC-Ge	1460, 975, 639, 532, 407	0.5	300	60	0.05–0.98	[48]
BDF	50GeO_2–50SiO_2: Bi (~100 ppm)	BAC-Ge	532	0.5	77, 300	40	0.35, 0.6	[48]
BEDF	SiO_2-Al_2O_3-Er_2O_3-Bi_2O_3 (~0.1 at%)	BAC-Al	532	0.06–0.16	300	55	0.05–0.15	[49]
BEDF	SiO_2-Al_2O_3-Er_2O_3-Bi_2O_3 (~0.1 at%)	BAC-Al	980, 830, 710, 633, 532	0.12	300	55	0–0.1	[49]
BEDF	SiO_2-Al_2O_3-GeO_2-P_2O_5-Er_2O_3-Bi_2O_3 (~0.1 at%)	BAC-Al	980	0.34	293–623	60	0–0.35	[52]
BDF	5P_2O_5–95SiO_2: Bi	BAC-P	407	1	300	30	0.53	[45]

Note: T, temperature of the fiber when it is irradiated by the laser.

Table 2.
Summary of photobleaching of BACs in BDFs and BEDFs.

here, **Table 2** summarizes a series of photobleaching of BACs observed in BDFs and BEDFs, along with their fiber compositions, BAC type, and irradiation conditions. The samples are doped with different compositions, such as Si, Ge, Al, P, Bi, and Er. The irradiation wavelengths are from 244 to 1460 nm, and the irradiation power varies from 0.005 to 1.5 MW/cm^2. The exposure temperature of the sample is in the range of 77–673 K.

In general, the bleaching ratio increases with irradiation intensity. Higher irradiation intensity provides more photons, leading to stronger photobleaching effect. It is worth noting that for both BAC-Si and BAC-Al, the bleaching ratio tends to saturate as the irradiation intensity increases [47, 52]. More interestingly, the photobleaching effect could happen under irradiation of some wavelengths even the irradiation intensity is quite small. However, for some irradiation wavelengths, even the irradiation intensity is large, there is still no obvious photobleaching phenomenon. For example, the luminescence of BAC-Si decays 20% after 830-nm irradiation with an intensity of 0.005 MW/cm^2 but has no change when exposed to 0.36 MW/cm^2 980-nm irradiation [47]. This indicates that the irradiation wavelength affects more on the photobleaching than the irradiation intensity.

The photobleaching effect significantly depends on the irradiation wavelength. As for BAC-Ge and BAC-Al, the photobleaching effect could happen by the irradiations at both resonant and nonresonant wavelengths, and larger bleaching ratio can be achieved by shorter irradiation wavelength [48, 49]. However, as for BAC-Si, only the wavelengths that are able to excite BAC-Si to the upper level could lead to the photobleaching [47]. According to **Table 2**, it is worth noting that irradiation wavelengths that can cause the photobleaching effect are always shorter than the luminescence peak wavelength of BACs. Therefore, it is supposed that the premise of photobleaching is that the photon energy for the photobleaching is larger than the excitation energy between the ground state and the first excited state of BACs.

Higher temperature evidently accelerates the electron movement rate. It is believed that the photobleaching of BACs is due to the electron escape. Therefore, the photobleaching of BACs becomes stronger at high temperatures, as demonstrated in [47, 48, 52, 54]. It is remarkable that for some irradiation wavelengths, the luminescence has little change at room temperature but is bleached significantly at higher temperatures [52, 54]. The increasing temperature provides enough thermal energy and assists the electron to flee from the BACs; however, the phonon energy is not sufficient for electron escape at room temperature.

8. Summary

Since the first observation of NIR luminescence in bismuth-doped glass, the bismuth-doped materials have attracted great attention due to their ultra-broadband luminescence. Especially, the bismuth-doped and bismuth/erbium co-doped optical fibers have been developed for the potential applications as optical amplifier and fiber laser. A number of researches have been taken focusing on the photostability of bismuth active center (BAC) in these BDFs/BEDFs. The results have demonstrated that the laser radiation can evidently cause the photobleaching of all types of BACs (BAC-Si, BAC-Ge, BAC-Al, and BAC-P), leading to the change of optical characteristics of the fiber. For BAC-Si, BAC-Ge, and BAC-Al, the photobleaching is much dependent upon the irradiation intensity, irradiation wavelength, and temperature. The recovery behavior of bleached BAC-Si and BAC-Ge can be achieved with the aid of phonon-assisted relaxation after the irradiation. It is noted that the BAC-Ge and BAC-Al can be bleached under irradiation at both resonant and nonresonant wavelengths; however, the photobleaching of BAC-Si can only

happen when the irradiation photon is able to excite the BAC-Si to the upper energy level. These differences indicate that the photobleaching of BACs is driven by multiple possible mechanisms. In bismuth-doped germanosilicate fiber, the possible mechanism of the photobleaching effect is the photoionization of GeODC, which participate in the formation of BAC-Ge. In addition, the fabrication process, material compositions, treatment conditions, as well as doping concentration of Si/Ge/Al/P have a great impact on the formation of their related ODCs (GeODC, AlODC, PODC, etc.) and ultimately affect the photobleaching of related BACs. All these investigations on photobleaching of BACs in these BDFs/BEDFs not only provide their photostability information but also give an insight to reveal the fundamental structure of BACs, which can be utilized to control the BACs in BDFs and BEDFs for the practical applications as an optical amplifier and fiber laser.

Acknowledgements

The authors are thankful for the support of National Natural Science Foundation of China (61520106014 and 61675032), Science and Technology Commission of Shanghai Municipality, China (SKLSFO2018-02) and 111 Project (D20031) and wish to express their thanks to other collaborators for their contributions.

Author details

Bowen Zhang[1], Mingjie Ding[1], Shuen Wei[1], Binbin Yan[2], Gang-Ding Peng[1], Yanhua Luo[1*] and Jianxiang Wen[3]

1 Photonics and Optical Communications, School of Electrical Engineering and Telecommunications, University of New South Wales, Sydney, NSW, Australia

2 State Key Laboratory of Information Photonics and Optical Communications, Beijing University of Posts and Telecommunications, Beijing, China

3 Key laboratory of Specialty Fiber Optics and Optical Access Networks, Joint International Research Laboratory of Specialty Fiber Optics and Advanced Communication, Shanghai University, Shanghai, China

*Address all correspondence to: yanhua.luo1@unsw.edu.au

References

[1] Murata K, Fujimoto Y, Kanabe T, Fujita H, Nakatsuka M. Bi-doped SiO_2 as a new laser material for an intense laser. Fusion Engineering and Design. 1999;**44**(1-4):437-439

[2] Denker B, Galagan B, Osiko V, Sverchkov S, Dianov E. Luminescent properties of Bi-doped boro-alumino-phosphate glasses. Applied Physics B. 2007;**87**(1):135-137

[3] Peng M, Dong G, Wondraczek L, Zhang L, Zhang N, Qiu J. Discussion on the origin of NIR emission from Bi-doped materials. Journal of Non-Crystalline Solids. 2011;**357**(11-13):2241-2245

[4] Peng M, Zollfrank C, Wondraczek L. Origin of broad NIR photoluminescence in bismuthate glass and Bi-doped glasses at room temperature. Journal of Physics. Condensed Matter. 2009;**21**(28):285106

[5] Ruan J, Su L, Qiu J, Chen D, Xu J. Bi-doped BaF_2 crystal for broadband near-infrared light source. Optics Express. 2009;**17**(7):5163-5169

[6] Suzuki T, Ohishi Y. Ultrabroadband near-infrared emission from Bi-doped Li_2O–Al_2O_3–SiO_2 glass. Applied Physics Letters. 2006;**88**(19):191912

[7] Zhou S, Dong H, Zeng H, Feng G, Yang H, Zhu B, et al. Broadband optical amplification in Bi-doped germanium silicate glass. Applied Physics Letters. 2007;**91**(6):061919

[8] Chu Y, Hu Q, Zhang Y, Gao Z, Fang Z, Liu L, et al. Topological engineering of photoluminescence properties of bismuth-or erbium-doped phosphosilicate glass of arbitrary P_2O_5 to SiO_2 ratio. Advanced Optical Materials. 2018;**6**(13):1800024

[9] Ahmad H, Shahi S, Harun SW. Bismuth-based erbium-doped fiber as a gain medium for L-band amplification and brillouin fiber laser. Laser Physics. 2010;**20**(3):716-719

[10] Bufetov I, Dianov E. Bi-doped fiber lasers. Laser Physics Letters. 2009;**6**(7):487

[11] Bufetov IA, Firstov SV, Khopin VF, Medvedkov OI, Guryanov AN, Dianov EM. Bi-doped fiber lasers and amplifiers for a spectral region of 1300-1470 nm. Optics Letters. 2008;**33**(19):2227-2229

[12] Bufetov IA, Melkumov MA, Firstov SV, Riumkin KE, Shubin AV, Khopin VF, et al. Bi-doped optical fibers and fiber lasers. IEEE Journal of Selected Topics in Quantum Electronics. 2014;**20**(5):111-125

[13] Dvoyrin V, Medvedkov O, Mashinsky V, Umnikov A, Guryanov A, Dianov E. Optical amplification in 1430-1495 nm range and laser action in Bi-doped fibers. Optics Express. 2008;**16**(21):16971-16976

[14] Luo Y, Wen J, Zhang J, Canning J, Peng G-D. Bismuth and erbium codoped optical fiber with ultrabroadband luminescence across O-, E-, S-, C-, and L-bands. Optics Letters. 2012;**37**(16):3447-3449

[15] Luo Y, Yan B, Zhang J, Wen J, He J, Peng G-D. Development of Bi/Er co-doped optical fibers for ultra-broadband photonic applications. Frontiers of Optoelectronics. 2018;**11**(1):37-52

[16] Wei S, Ding M, Fan D, Luo Y, Wen J, Peng G-D. Effects of post treatments on bismuth-doped and bismuth/erbium co-doped optical fibres. Bismuth: Advanced Applications and Defects Characterization. 2018;**155**

[17] Firstov S, Khopin V, Bufetov I, Firstova E, Guryanov A,

Dianov E. Combined excitation-emission spectroscopy of bismuth active centers in optical fibers. Optics Express. 2011;**19**(20):19551-19561

[18] Sathi ZM, Zhang J, Luo Y, Canning J, Peng G. Spectral properties and role of aluminium-related bismuth active Centre (BAC-Al) in bismuth and erbium co-doped fibres. Optical Materials Express. 2015;**5**(5):1195-1209

[19] Firstov SV, Alyshev SV, Riumkin KE, Khegai AM, Kharakhordin AV, Melkumov MA, et al. Laser-active fibers doped with bismuth for a wavelength region of 1.6-1.8 μm. IEEE Journal of Selected Topics in Quantum Electronics. 2018;**24**(5):1-15

[20] Wen J, Liu W, Dong Y, Luo Y, Peng G-D, Chen N, et al. Radiation-induced photoluminescence enhancement of Bi/Al-codoped silica optical fibers via atomic layer deposition. Optics Express. 2015;**23**(22):29004-29013

[21] Firstov S, Alyshev S, Khopin V, Melkumov M, Guryanov A, Dianov E. Photobleaching effect in bismuth-doped germanosilicate fibers. Optics Express. 2015;**23**(15):19226-19233

[22] Firstov SV, Alyshev SV, Khopin VF, Kharakhordin AV, Lobanov AS, Firstova EG, et al. Effect of heat treatment parameters on the optical properties of bismuth-doped GeO_2: SiO_2 glass fibers. Optical Materials Express. 2019;**9**(5):2165-2174

[23] Wei S, Luo Y, Ding M, Cai F, Xiao G, Fan D, et al. Thermal effect on attenuation and luminescence of Bi/Er co-doped fiber. IEEE Photonics Technology Letters. 2016;**29**(1):43-46

[24] Wei S, Luo Y, Fan D, Xiao G, Chu Y, Zhang B, et al. BAC activation by thermal quenching in bismuth/erbium codoped fiber. Optics Letters. 2019;**44**(7):1872-1875

[25] Zhang B, Wei S, Khan MTA, Luo Y, Peng G-D. Dynamics study of thermal activation of BAC-Si in bismuth/erbium-codoped optical fiber. Optics Letters. 2020;**45**(2):571-574

[26] Song L, Hennink E, Young IT, Tanke HJ. Photobleaching kinetics of fluorescein in quantitative fluorescence microscopy. Biophysical Journal. 1995;**68**(6):2588-2600

[27] Greenbaum L, Rothmann C, Lavie R, Malik Z. Green fluorescent protein photobleaching: A model for protein damage by endogenous and exogenous singlet oxygen. Biological Chemistry. 2000;**381**(12):1251-1258

[28] Krebs J, Segal C, Yen W, Happek U. Photo bleaching in Sm^{2+} selectively doped epitaxial CaF_2 films. Journal of Luminescence. 1997;**72**:220-221

[29] Pollnau M, Hardman P, Clarkson W, Hanna D. Upconversion, lifetime quenching, and ground-state bleaching in Nd^{3+}: $LiYF_4$. Optics Communication. 1998;**147**(1-3):203-211

[30] Takeshita S, Ogata H, Isobe T, Sawayama T, Niikura S. Effects of citrate additive on transparency and photostability properties of YVO_4: Bi^{3+}, Eu^{3+} nanophosphor. Journal of the Electrochemical Society. 2010;**157**(3):J74-J80

[31] Busch G, Greve K, Olson G, Jones R, Rentzepis P. Photobleaching and recovery times of the mode-locking dye DODCI. Chemical Physics Letters. 1975;**33**(3):412-416

[32] Oster G, Wotherspoon N. Photobleaching and photorecovery of dyes. The Journal of Chemical Physics. 1954;**22**(1):157-158

[33] Saylor J. Photobleaching of disodium fluorescein in water. Experiments in Fluids. 1995;**18**(6):445-447

[34] Mills A, Wang J. Photobleaching of methylene blue sensitised by TiO_2: An ambiguous system? Journal of Photochemistry and Photobiology, A: Chemistry. 1999;**127**(1-3):123-134

[35] Henderson JN, H-w A, Campbell RE, Remington SJ. Structural basis for reversible photobleaching of a green fluorescent protein homologue. Proceedings of the National Academy of Sciences. 2007;**104**(16):6672-6677

[36] Sinnecker D, Voigt P, Hellwig N, Schaefer M. Reversible photobleaching of enhanced green fluorescent proteins. Biochemistry. 2005;**44**(18):7085-7094

[37] White J, Stelzer E. Photobleaching GFP reveals protein dynamics inside live cells. Trends in Cell Biology. 1999;**9**(2):61-65

[38] Chávez AG, Kir'Yanov A, Barmenkov YO, Il'Ichev N. Reversible photo-darkening and resonant photo-bleaching of ytterbium-doped silica fiber at in-core 977-nm and 543-nm irradiation. Laser Physics Letters. 2007;**4**(10):734

[39] Manek-Hönninger I, Boullet J, Cardinal T, Guillen F, Ermeneux S, Podgorski M, et al. Photodarkening and photobleaching of an ytterbium-doped silica double-clad LMA fiber. Optics Express. 2007;**15**(4):1606-1611

[40] Gebavi H, Taccheo S, Tregoat D, Monteville A, Robin T. Photobleaching of photodarkening in ytterbium doped aluminosilicate fibers with 633 nm irradiation. Optical Materials Express. 2012;**2**(9):1286-1291

[41] Laperle P, Chandonnet A, Vallée R. Photobleaching of thulium-doped ZBLAN fibers with visible light. Optics Letters. 1997;**22**(3):178-180

[42] Savelyev E, Butov O, Yapaskurt V, Golant K. Near-infrared luminescence of bismuth in silica-based glasses with different additives. Journal of Communications Technology and Electronics. 2018;**63**(12):1458-1468

[43] Vtyurina D, Romanov A, Kuznetsov M, Fattakhova Z, Khaula E, Lisitskii I, et al. Optical properties of bismuth-doped $TlCdCl_3$ crystal. Russian Journal of Physical Chemistry B. 2016;**10**(1):1-4

[44] Wang X, Xu S, Yang Z, Peng M. Ultra-broadband red to NIR photoemission from multiple bismuth centers in $Sr_2B_5O_9Cl$: Bi crystal. Optics Letters. 2019;**44**(19):4821-4824

[45] Firstov SV, Alyshev SV, Kharakhordin AV, Riumkin KE, Dianov EM. Laser-induced bleaching and thermo-stimulated recovery of luminescent centers in bismuth-doped optical fibers. Optical Materials Express. 2017;**7**(9):3422-3432

[46] Ding M, Wei S, Luo Y, Peng G-D. Reversible photo-bleaching effect in a bismuth/erbium co-doped optical fiber under 830 nm irradiation. Optics Letters. 2016;**41**(20):4688-4691

[47] Ding M, Fang J, Luo Y, Wang W, Peng G-D. Photo-bleaching mechanism of the BAC-Si in bismuth/erbium co-doped optical fibers. Optics Letters. 2017;**42**(24):5222-5225

[48] Firstov SV, Alyshev SV, Firstova EG, Melkumov MA, Khegay AM, Khopin VF, et al. Dependence of the photobleaching on laser radiation wavelength in bismuth-doped germanosilicate fibers. Journal of Luminescence. 2017;**182**:87-90

[49] Zhao Q, Luo Y, Tian Y, Peng G-D. Pump wavelength dependence and thermal effect of photobleaching of BAC-Al in bismuth/erbium codoped aluminosilicate fibers. Optics Letters. 2018;**43**(19):4739-4742

[50] Ding M, Luo Y, Wen J, Peng G-D, editors. Dynamic behavior of pump

light radiation induced photo-bleaching effect on BAC-Si in bismuth/erbium co-doped optical fibers. In: Fiber Lasers XV: Technology and Systems. Washington, D.C., USA: International Society for Optics and Photonics; 2018

[51] Firstov S, Alyshev S, Melkumov M, Riumkin K, Shubin A, Dianov E. Bismuth-doped optical fibers and fiber lasers for a spectral region of 1600-1800 nm. Optics Letters. 2014;**39**(24):6927-6930

[52] Zhang B, Luo Y, Ding M, Wei S, Fan D, Xiao G, et al. Thermally aggravated photo-bleaching of BAC-Al in bismuth/erbium co-doped optical fiber. Optics Letters. 2019;**44**(19):4829-4832

[53] Firstov S, Firstova E, Alyshev S, Khopin V, Riumkin K, Melkumov M, et al. Recovery of IR luminescence in photobleached bismuth-doped fibers by thermal annealing. Laser Physics. 2016;**26**(8):084007

[54] Alyshev S, Kharakhordin A, Firstova E, Khegai A, Melkumov M, Khopin V, et al. Photostability of laser-active centers in bismuth-doped GeO_2–SiO_2 glass fibers under pumping at 1550 nm. Optics Express. 2019;**27**(22):31542-31552

[55] Johnston D. Stretched exponential relaxation arising from a continuous sum of exponential decays. Physical Review B. 2006;**74**(18):184430

[56] Zhang B, Wei S, Chu Y, Talal M, Fu X, Yan B, et al., editors. Thermal quenching effect on BAC-P in bismuth/erbium co-doped optical fibre. In: Asia Communications and Photonics Conference. Washington, D.C., USA: Optical Society of America; 2019

[57] Zhao Q, Luo Y, Hao Q, Peng G-D. Effect of thermal treatment parameters on the spectral characteristics of BAC-Al in bismuth/erbium-codoped aluminosilicate fibers. Optics Letters. 2019;**44**(18):4594-4597

[58] Xu H, Yan B, Lin J, Luo Y, Lu P, Wang K, et al. Effects of quenching and cooling upon near infrared luminescence of Bi/Er co-doped optical fiber. Optical Materials Express. 2019;**9**(7):3156-3168

[59] Kharakhordin A, Alyshev S, Firstova E, Khegai A, Melkumov M, Khopin V, et al. Analysis of thermally activated processes in bismuth-doped GeO_2-SiO_2 glass fibers using the demarcation energy concept. Optical Materials Express. 2019;**9**(11):4239-4246

[60] Hosono H, Abe Y, Kinser DL, Weeks RA, Muta K, Kawazoe H. Nature and origin of the 5-eV band in SiO_2: GeO_2 glasses. Physical Review B. 1992;**46**(18):11445

[61] Dianov EM. Nature of Bi-related near IR active centers in glasses: State of the art and first reliable results. Laser Physics Letters. 2015;**12**(9):095106

[62] Dianov EM. On the nature of near-IR emitting Bi centres in glass. Quantum Electronics. 2010;**40**(4):283

[63] Vasil'ev SA, Dianov EM, Koltashev VVE, Marchenko VM, Mashinsky VM, Medvedkov OI, et al. Photoinduced changes in the Raman spectra of germanosilicate optical fibres. Quantum Electronics. 1998;**28**(4):330